URSI GASS 2021, Rome, Italy, 28 August - 4 September 2021

Night-time Ionospheric Localized Enhancements (NILE) Observed in North America Following Geomagnetic Disturbances

Alex T. Chartier[(1)], Seebany Datta-Barua[(2)], and Sarah E. McDonald[(2)]
(1) Johns Hopkins University/Applied Physics Laboratory, Laurel, MD 20723
(2) Mechanical, Materials, and Aerospace Engineering Department, Illinois Institute of Technology, Chicago, IL 60616
(3) Space Science Division, Naval Research Laboratory, Washington, DC 20375

Abstract

The Ionospheric Data Assimilation Four-Dimensional (IDA4D) technique has been coupled to Sami3 is Another Model of the Ionosphere (SAMI3). In this application, ground- and space-based GPS Total Electron Content (TEC) data have been assimilated into SAMI3 while *in situ* electron densities, autoscaled ionosonde NmF2 and reference GPS stations have been used for validation. IDA4D/SAMI3 shows that Night-time Ionospheric Localized Enhancements (NILE) are formed following geomagnetic storms in November 2003 and August 2018. The NILE phenomenon appears as a moderate, longitudinally extended enhancement of NmF2 at 30-40° N MLAT, occurring in the late evening (20-24 LT) following much larger enhancements of the equatorial anomaly crests in the main phase of the storms. The NILE appears to be caused by upward and northward plasma transport around the dusk terminator, which is consistent with eastward polarization electric fields. Independent validation confirms the presence of the NILE, and indicates that IDA4D is effective in correcting random errors and systematic biases in SAMI3. In all cases, biases and root-mean-square errors are reduced by the data assimilation, typically by a factor of 2 or more. During the most severe part of the November 2003 storm, the uncorrected ionospheric error on a GPS 3D position at 1LSU (Louisiana) is estimated to exceed 34 m. The IDA4D/SAMI3 specification is effective in correcting this down to 10-m.

1 Introduction

Nighttime Ionospheric Localized Enhancements (NILE) have been observed at northern mid-latitudes during the recovery phase of major storms and superstorms (Datta-Barua, 2004; Datta-Barua et al., 2008), notably 31 October and 20 November 2003. The NILE constitutes a major enhancement of the ionosphere relative to the background nighttime ionosphere, in a latitudinally narrow channel extending from the south-east to the northwest. In all cases observed to date, the NILE appears to originate above the Caribbean and extends into the continental USA. This phenomenon is not currently understood. State-of-the-art physics models account for many important electrodynamic and chemical effects, and have been shown to be able to model the SED. However global models have not, to date, captured the localized nature of the NILE. We seek to address the improvement in modeling the plasma density of the NILE using data assimilation.

2 Method

This investigation uses assimilation of GPS-derived TEC data (the IDA4D technique) to correct a first-principles ionospheric model (SAMI3) in order to produce three-dimensional, time-dependent images of electron density during two ionospheric storms. The primary case is 20-21 November 2003, which is the most recent ionospheric superstorm. The storm of 25 – 26 August 2018 is chosen as a comparison case because it has good data coverage and covers a moderately intense geomagnetic disturbance. For validation, we use independent GPS stations, ionosonde data and *in situ* density data from the CHAMP satellite.

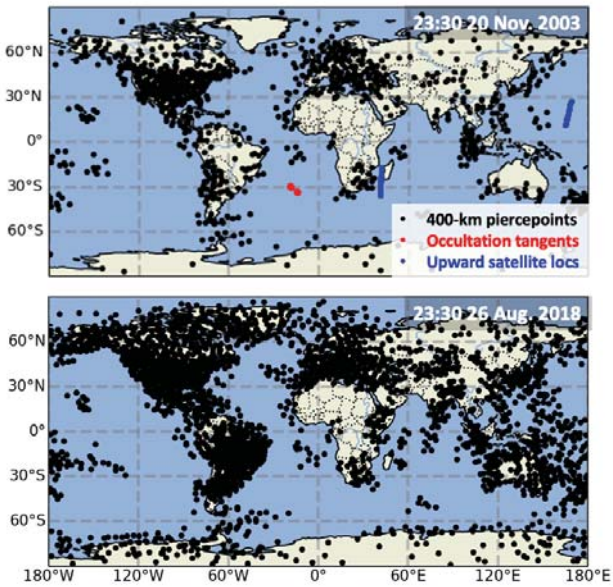

Figure 1 shows the data assimilated in a single five-minute assimilation step centered on 23:30 UT on 20 November 2003 and 26 August 2018. 400-km piercepoints of ground-to-space GPS TEC data are in black. Tangent points of radio occultation data are in red. Locations of satellites taking upward GPS TEC measurements are in blue.

3 Results

The evolution of the November 2003 storm, as captured by IDA4D/SAMI3, is shown in Figure 2. This data shows an enormous enhancement of NmF2 up to 2E13 el. m^3 at 21 UT. Note that this enhancement occurs much later in local time than might be expected, covering the region approximately 0-80 W (16-24 LT).

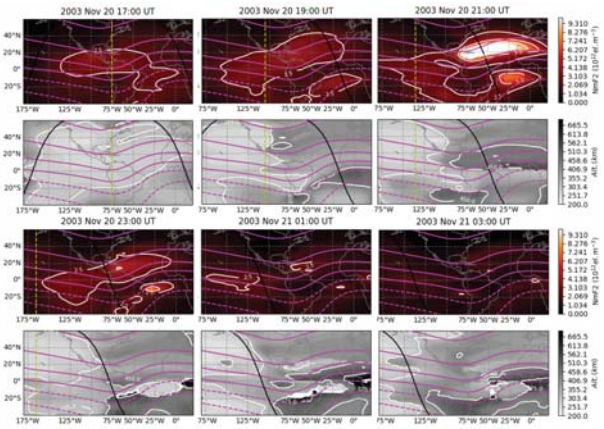

Figure 2: Evolution of the November 2003 storm as captured by IDA4D/SAMI3. NmF2 is in the upper panels in color, while hmF2 is in greyscale in the lower panels. NmF2 contours are spaced by 2.5×10^{12} el. m^{-3} (starting at 2×10^{12} el. m^{-3}) while hmF2 contours are spaced by 125 km of altitude. Panels cover 18:30 – 23:30 UT at hourly intervals. Local noon is shown as a yellow dashed line.

IDA4D/SAMI3 indicates a huge enhancement of the equatorial ionization anomaly in the late evening sector, peaking at 2×10^{12} el. m^{-3} at 21:00 UT. This is accompanied by a dramatic uplift of the ionospheric peak height up to 711 km at 21:30 UT, close to the equator between the anomaly crests. This supercharging of the "fountain" effect is responsible for the enhanced NmF2 poleward of the uplift region. A remarkable feature of this storm as it evolves temporally is that the northern enhanced EIA crest remains in the same longitude sector for >5 hours, effectively "stuck" above the Caribbean with a peak around 70 W. The IDA4D/SAMI3 model output shown in Figure 3 indicates this NILE event.

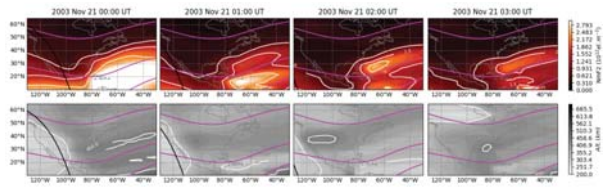

Figure 3: Night-time ionospheric localized enhancements (NILE) in the American sector following the November 2003 storm, as estimated by IDA4D/SAMI3. Upper: NmF2 in color and white contours, lower: hmF2 in greyscale and white contours. International Geomagnetic Reference Field contours are shown in magenta.

4 Validation

The CHAMP *in situ* density dataset allows for direct validation of the NILE phenomenon seen around 3:00 UT on 20 November 2003. Data from CHAMP's successor, Swarm, are available to validate the August 2018 case, though the relevant pass is too early to see the NILE on that day. Note that these data are not used by IDA4D in this case, so the output in Figure 4 is an independent validation. On 21 November 2003, CHAMP passed approximately along the 60 W meridian at 455 km altitude, moving from south to north between 2:25 and 3:00 UT. The NILE enhancement around 30° N is clearly visible in CHAMP and in IDA4D/SAMI3, as are the other major features of both plots – notably the northern EIA crest around 15° N and the southern crest between 35-50° S. These features are either absent or distorted in the standalone SAMI3 output. In the August 2018 case, IDA4D/SAMI3 also greatly improves agreement between model and data.

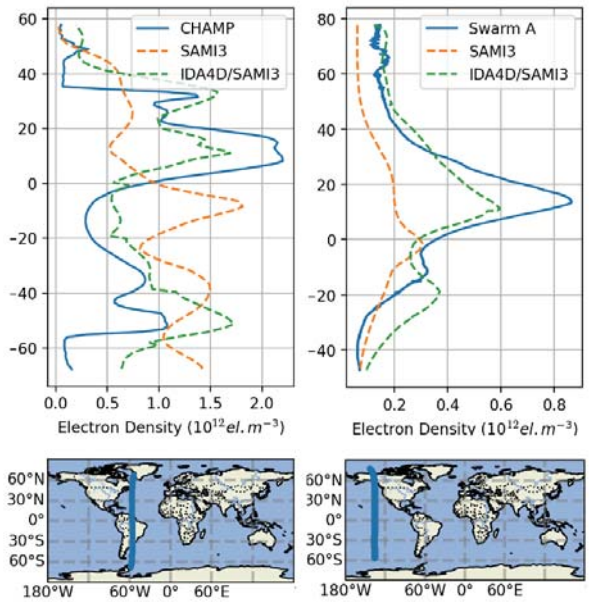

Figure 4: Validation of IDA4D/SAMI3 and SAMI3 against *in situ* electron density data from CHAMP (~450-km) and Swarm A (~425-km) from 2:25-3:00 UT on 21 November 2003 and 23:15-23:50 UT on 25 August 2018 respectively. The results indicate that IDA4D/SAMI3 performs much better than SAMI3 in reproducing the major features of the independent CHAMP and SWARM *in situ* data.

The November 2003 storm case is also validated in terms of ionospheric errors on 3D GPS position. This is achieved as follows:

First, the ionospheric range error on single-frequency GPS is calculated based on the dual-frequency TEC data observed by the reference GPS stations.

Second, a correction is applied based on the model (either IDA4D/SAMI3 or SAMI3).

Finally, an inversion is performed to estimate the 3D position of the test receivers, based on the observed

ionospheric delays and the modeled corrections. This is compared against the known true position of the test receivers.

The observed range, d_{obs}, is calculated by adding the true distance between the ith satellite position, $\boldsymbol{tx_i}$, based on precise orbit files) and receiver, $\boldsymbol{d}_{true}$, and the delay in meters due to slant Total Electron Content (sTEC) between the satellite and receiver, d_{iono}. At L1 (1575.42 MHz), the following applies:

$$d_{iono} = \text{sTEC} / 6.13 \quad (1)$$

where sTEC is in TEC units (10^{16} el. m^{-3}). From these simulated ranges, the single-frequency position estimate, $\boldsymbol{rx}_{est}$, can be obtained by minimizing a cost function. In that cost function, the satellite's elevation angle, e, is used as a scaling factor to prioritize fitting to satellites overhead rather than at low angles, where ionospheric and other errors are typically much larger:

$$\boldsymbol{rx}_{est} = arg.min.\sum_i\left((\boldsymbol{rx} - \boldsymbol{tx_i})^2 - {d_{obs\,i}}^2\right)^2 . e \quad (2)$$

The 3D GPS position validation for November 2003 is shown in Figure 5, covering the AMC2 and 1LSU reference stations.

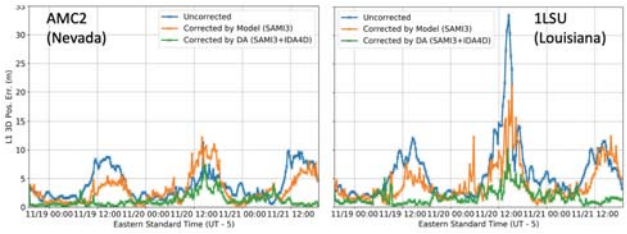

Figure 5: Ionospheric errors on 3D GPS position at AMC2 and 1LSU reference stations, based on uncorrected observed TEC, SAMI3-corrected TEC and IDA4D/SAMI3-corrected TEC.

Uncorrected ionospheric errors on 3D position at the two stations are estimated to have exceeded 34 m in magnitude at 1LSU at the peak of the storm. These errors are reduced to a maximum 10m error at the peak of the storm by IDA4D/SAMI3. Note that the data assimilation is critical to this performance improvement – SAMI3 without data assimilation at best provides only a modest improvement and in some cases makes the positioning solution worse (e.g. at AMC2 on 20 November).

5 Discussion

The new coupled IDA4D/SAMI3 model provides insights into the NILE phenomenon. The results of this new technique show night-time (20-24 LT) ionospheric electron density enhancements between 30-40° N MLAT in the aftermath of a great storm (November 2003) and a strong storm (August 2018). In both cases, the plasma source for these enhancements appears to be the storm-enhanced northern equatorial ionization anomaly crest, though there are some important differences between the two events. Independent validation indicates that the IDA4D/SAMI3 results are reliable.

6 Conclusions

The newly-coupled IDA4D/SAMI3 shows the NILE occurring after storms in November 2003 and August 2018. The phenomenon appears as a moderate, longitudinally extended enhancement of NmF2 at 30-40° N, occurring in the late evening (20-24 LT) following much larger enhancements of the equatorial anomaly crests in the main phase of the storm. Electric field effects related to the "superfountain" and the polarization at the terminator appear to be the cause of these enhancements. Validation against independent *in situ* density data, autoscaled ionosonde NmF2 data and reference GPS data indicates that IDA4D is effective in correcting biases present in SAMI3. The impact can be 35-50% reductions in root-mean-square NmF2 errors, and up to 70% improvement in GPS positioning estimates.

6 Acknowledgements

The authors acknowledge the support of NASA LWS-TRT grant NNH17ZDA001N-LWS. Geophysical indices obtained from NASA OMNI: omniweb.gsfc.nasa.gov/
Ground GPS data obtained from millstonehill.haystack.mit.edu/ courtesy of Anthea Coster. Raw data are available from the International GNSS Service. CHAMP and GRACE data obtained from isdc.gfz-potsdam.de/
Ionosonde data were obtained from giro.uml.edu/didbase/scaled.php
The pyIGRF wrapper was used to generate geomagnetic coordinates: pypi.org/project/pyIGRF/
Davitpy was used to plot the solar terminator: https://github.com/vtsuperdarn/davitpy

7 References

Bust, G. S., Garner, T. W., & Gaussiran, T. L. (2004). Ionospheric Data Assimilation Three-Dimensional (IDA3D): A global, multisensor, electron density specification algorithm. *Journal of Geophysical Research: Space Physics*, *109*(A11).

Buonsanto, M. J. (1999). Ionospheric storms—A review. *Space Science Reviews*, *88*(3-4), 563-601.

Collins, N., G. Theurich, C. DeLuca, M. Suarez, A. Trayanov, V. Balaji, P. Li, W. Yang, C. Hill, and A. da Silva (2005). Design and Implementation of Components in the Earth System Modeling Framework. International Journal of High Performance Computing Applications, Volume 19, Number 3, pp. 341-350.

Datta-Barua, S. (2004, September). Ionospheric threats to space-based augmentation system development. In *Proc. ION GNSS 2004* (pp. 21-24).

Datta-Barua, S., Mannucci, A. J., Walter, T., and Enge, P., "Altitudinal variation of midlatitude localized TEC enhancement from ground- and space-based measurements," *Space Weather*, 6, S10D06, 2008, doi:10.1029/2008SW000396.

Drob, D. P., Emmert, J. T., Meriwether, J. W., Makela, J. J., Doornbos, E., Conde, M., et al. (2015). An update to the Horizontal Wind Model (HWM): The quiet time thermosphere. Earth and Space Science, 2, 301–319. https://doi.org/10.1002/2014EA000089

Fejer, B. G., J. W. Jensen, T. Kikuchi, M. A. Abdu, and J. L. Chau (2007), Equatorial Ionospheric Electric Fields During the November 2004 Magnetic Storm, J. Geophys. Res., 112, A10304, doi:10.1029/2007JA012376.

Foster, J. C., & Erickson, P. J. (2013). Ionospheric superstorms: Polarization terminator effects in the Atlantic sector. *Journal of Atmospheric and Solar-Terrestrial Physics*, *103*, 147-156.

Galkin, I. A., Khmyrov, G. M., Kozlov, A. V., Reinisch, B. W., Huang, X., & Paznukhov, V. V. (2008, February). The Artist 5. In *AIP Conference Proceedings* (Vol. 974, No. 1, pp. 150-159). American Institute of Physics.

Hardy, D. A., Gussenhoven, M. S., & Holeman, E. (1985). A statistical model of auroral electron precipitation. Journal of Geophysical Research, 90(A5), 4229–4248.

Hardy, D. A., Gussenhoven, M. S., & Brautigam, D. (1989). A statistical model of auroral ion precipitation. Journal of Geophysical Research, 94(A1), 370–392.

Huba, J. D., Joyce, G., & Fedder, J. A. (2000). Sami2 is Another Model of the Ionosphere (SAMI2): A new low-latitude ionosphere model. *Journal of Geophysical Research: Space Physics*, *105*(A10), 23035-23053.

Huba, J. D., Joyce, G., & Krall, J. (2008). Three-dimensional equatorial spread F modeling. Geophysical Research Letters, 35, L19106. https://doi.org/10.1029/2009GL040284

Huba, J. D., and Sazykin, S. (2014), "Storm time ionosphere and plasmasphere structuring: SAMI3-RCM simulation of the 31 March 2001 geomagnetic storm," *Geophysical Research Letters*, Vol. 41, No. 23, pp. 8208-8214.

Ippolito, A., Altadill, D., Scotto, C., & Blanch, E. (2018). Oblique Ionograms Automatic Scaling Algorithm OIASA application to the ionograms recorded by Ebro observatory ionosonde. *Journal of Space Weather and Space Climate*, *8*, A10.

Loewe, C. A., & Prolss, G. W. (1997). Classification of mean behavior of magnetic storms. *Journal of Geophysical Research*, **102**(A7), 14,209–14,213. https://doi.org/10.1029/96JA04020

Mannucci, A. J., B. T. Tsurutani, B. A. Iijima, A. Komjathy, A. Saito, W. D.Gonzalez, F. L. Guarnieri, J. U. Kozyra, and R. Skoug (2005), Dayside global ionospheric response to the major interplanetary events of October29 – 30, 2003 ''Halloween storms,'' Geophys. Res. Lett., 32, L12S02,doi:10.1029/2004GL021467

Picone, J. M., Hedin, A. E., Drob, D. P., & Aikin, A. C. (2002). NRLMSISE-00 empirical model of the atmosphere: Statistical comparisons and scientific issues. Journal of Geophysical Research, 107(A12), 1468. https://doi.org/10.1029/2002JA009430

Richmond, A.D., (1995). Ionospheric electrodynamics using magnetic apex coordinates. *Journal of geomagnetism and geoelectricity*, *47*(2), 191-212.

Tsurutani, B. T., Verkhoglyadova, O. P., Mannucci, A. J., Saito, A., Araki, T., Yumoto, K., ... & McCreadie, H. (2008). Prompt penetration electric fields (PPEFs) and their ionospheric effects during the great magnetic storm of 30–31 October 2003. *Journal of Geophysical Research: Space Physics*, *113*(A5).

Weimer, D. R. (2005). Predicting surface geomagnetic variations using ionospheric electrodynamic models. Journal of Geophysical Research, 110, A12307. https://doi.org/10.1029/2005JA011270